# Improving Ion Mobility Measurement Sensitivity by Utilizing Helium in an Ion Funnel Trap

Yehia M. Ibrahim,* Sandilya V. B. Garimella, Aleksey V. Tolmachev, Erin S. Baker, and Richard D. Smith

Biological Sciences Division, Pacific Northwest National Laboratory, P.O. Box 999, Richland, Washington 99352, United States

S *Supporting Information*

ABSTRACT: Ion mobility instruments that utilize nitrogen as buffer gas are often preceded by an ion trap and accumulation region that also uses nitrogen, and for different inert gases, no significant effects upon performance are expected for ion mobility spectrometry (IMS) of larger ions. However, we have observed significantly improved performance for an ion funnel trap upon adding helium; the signal intensities for higher m/z species were improved by more than an order of magnitude compared to using pure nitrogen. The effect of helium upon IMS resolving power was also studied by introducing a He/N_2 gas mixture into the drift cell, and in some cases, a slight improvement was observed compared to pure N_2. The improvement in signal can be largely attributed to faster and more efficient ion ejection into the drift tube from the ion funnel trap.
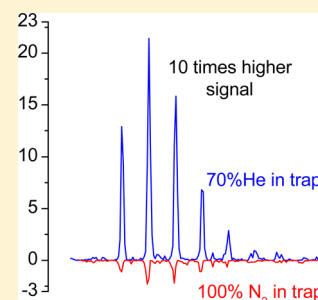
Ion mobility spectrometry (IMS) is a gas phase separation technique in which ions are distinguished according to their collision cross sections.[1] Ion packets are pulsed into a drift cell that contains a buffer gas and pulled by a uniform weak electric field. The measured ion arrival time is inversely proportional to the ion's mobility which is in turn inversely proportional to its collision cross section.[2] IMS has achieved significant interest for its potential to augment analytical applications of mass spectrometry (MS), as well as for more fundamental applications, e.g., where collision cross sections can be used to probe the geometry of candidate structures by comparing the measured cross section to the calculated one for different candidate structures. Helium is usually used as a buffer gas due to the extensive data available and the well-developed models that describe ion-He interaction. Since He cannot rotate or vibrate, has no dipole, and is the least polarizable of all atoms and molecules, it is the simplest system for which to model mobilities, making it generally preferred for structural elucidation by IMS.

However, nitrogen is also used widely as a buffer gas due to its broad availability in high purity and low cost.[3] In addition, other gases such as carbon dioxide and argon have also been utilized to affect the separation power of IMS.[4] To initiate an IMS experiment, ion packets are usually generated from a pulsed source (e.g., MALDI)[5] or continuous source[6] (e.g., ESI) by chopping the ion beam using a Bradbury-Nielsen gate[7] or mechanical chopper.[8] To improve the IMS duty cycle and sensitivity with continuous sources, ion accumulation and trapping have been used prior to injecting ions into the drift cell.[9] Traditionally, ion traps that precede drift cell use the same buffer gas composition as the drift cell, proving ease of IMS design and convenience in arranging the ion source relative to the drift cell.

Our laboratory has developed a sensitive IMS-MS platform that generally utilizes nitrogen as the buffer gas.[10,11] The ion source in this instrument contains an ion funnel trap (IFT) which efficiently traps and releases ions into the drift cell.[10,12] The IFT is a stacked-ring electrode RF ion guide that confines ions radially by applying a 180° out-of-phase RF waveform to adjacent ring-electrodes. Axial confinement is achieved by applying appropriate DC potentials to entrance and exit grids. The IFT is typically operated at ~4 Torr utilizing nitrogen gas flowing from the drift cell. Utilizing the IFT with the IMS drift cell has been shown to provide improved ion utilization efficiency and is a cornerstone to the overall high sensitivity of the platform.[10] In this work, we observed that introducing helium into the IFT region while operating the drift cell with nitrogen further improved the sensitivity of the platform, in some cases by more than an order of magnitude. We show in the manuscript that this improvement is attributed to the expedited ejection of ions from the trap.

EXPERIMENTAL SECTION

The instrument utilized in the experiment consists of a home-built ion mobility spectrometer (IMS) coupled to a commercial quadrupole time-of-flight mass spectrometer (model 6538 QTOF, Agilent technologies, Santa Clara, CA, USA). The layout of the IMS platform is shown in Figure 1. Ions are formed by electrospray using a 20 μm i.d. fused-silica emitter into a heated metal capillary inlet (500 μm i.d., 6 cm long). The atmospheric side of the inlet capillary is housed behind a curtain plate orifice where a curtain gas flows in-between the inlet capillary and the curtain plate. The curtain gas as well as the buffer gas (to the drift cell) is supplied through flow controllers (1479A and 247D power supply/readout, MKS Instruments, Andover MA, USA) which precisely control the
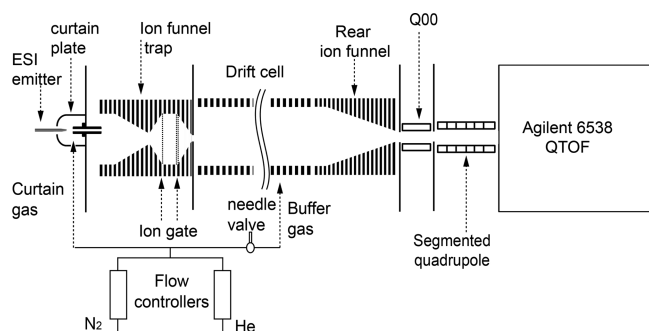
Figure 1. Schematic showing the IMS-QTOF MS platform.

flow of each gas (He or N_2). The inlet capillary as well as the curtain gas is heated to 120 °C. Ions exiting the inlet capillary are captured using an ion funnel trap (IFT).[10,12] The design of the ion funnel trap is similar to that previously described[12] with the exception that the electrodes are currently made using printed-circuit-boards (PCBs) instead of brass and that the electrical components (capacitors and resistors) are mounted on each PCB electrode while connections between adjacent electrodes are made through miniature spring-loaded connectors. The PCBs simplify the construction of the IFT, improve its robustness, and significantly lower the total capacitance, and thus, less power is needed to provide the required RF potential. Details on the IFT are presented in the Supporting Information. The inlet capillary is offset relative to the center axis of the ion funnel trap to minimize neutrals contamination of downstream ion optics. Offsetting the inlet capillary also reduces gas dynamic effects that can disturb ion trapping. The expanded ion plume is focused and accumulated inside the ion trap for typically 1−20 ms out of a 60 ms IMS cycle time (i.e., the time before the introduction of the next pulse of ions). RF frequency of 1 MHz and amplitude of 150 V_{p-p} is applied to the IFT. Ions are typically released from the trap by lowering the voltage on the exit grid for ~300−500 μs. The released ion packet is radially focused in the converging portion of the IFT and then injected into the drift cell. The drift cell is 82 cm long and consists of drift rings of 50 mm i.d./70 mm o.d. and spaced 5 mm apart. Similar to the IFT electrodes, the drift rings are also made using PCB materials. In the IFT, a metalized 2 mm wide ring encompasses the inside circular edge of the electrode, but for the drift rings, the whole ring is metalized to ensure a homogeneous field and to minimize ground potential penetration. Following the drift cell is a rear ion funnel that has entrance electrodes of 50 mm i.d. to capture diffused ion packets after traveling through the drift cell; the rear ion funnel is 12 cm long, resulting in a total effective drift tube length of 94 cm. Ions exit this rear ion funnel through a 3 mm i.d. conductance limiting orifice and are transmitted through two differentially pumped regions that host two quadrupoles. A DC gradient of ~18 V/cm is applied to the drift cell and rear ion funnel, which is filled with N_2 gas to 4 Torr. Pressure in the drift cell is maintained slightly higher (~50 mTorr) than the source to reduce contamination from the source region or alteration of the drift tube gas composition. The pressure in the interface of the ion source as well as the drift cell is measured using capacitance manometers (627B Baratron, MKS Instruments Inc., Andover MA USA). Following the drift cell, the quadrupole is segmented to allow application of a DC gradient to the segments and thus minimize ion residence time and any contributions to mobility

measurements. Ions are then transmitted through the Agilent QTOF interface and detected. Signal from the Agilent TOFMS detector was fed into a 1 GS/s 8-bit AP240 analog-to-digital converter (ADC) board (Acqiris, Geneva, Switzerland) and processed by a custom-built acquisition and control software written in C#.

Ion trajectory simulations were performed using SIMION 8.1 (Scientific Instrument Services Inc., Ringoes, NJ, USA). The effects of the DC voltages, collisions with the buffer gas, and the RF on the ion trajectories were incorporated into SIMION with a user defined code. The collisions of ions with buffer gas at 4 Torr were simulated using the statistical diffusion simulation (SDS) model.[13] Ion−ion interactions were considered assuming the columbic repulsion for 10^7 charges of 784 m/z ($z = 2$).

The sample used in this work was prepared by proteolytic digestion of bovine serum albumin (BSA; Pierce Biotechnology, Rockford, IL, USA) using sequencing grade trypsin (Promega, Madison, WI, USA) and previously described procedures.[14] The resulting solution was then diluted to 0.2 μg/μL in a 49.5:49.5:1 methanol/water/acetic acid buffer.

■ RESULTS AND DISCUSSION

The detailed effects of utilizing helium (He) in various regions of an IMS-MS platform have been examined in this work. Utilizing He as a buffer gas can potentially have an impact on the performance of the front and rear ion funnels, the ion accumulation and injection trap, and the drift cell. To isolate the effects of He on the different components of the IMS-MS platform, the ion funnel trap (IFT) was initially turned off and ions from the source were continuously transmitted through the ESI-MS interface, the entire IMS drift cell, and the IMS-MS interface. This continuous ion beam allowed evaluation of He effects on the ion funnel transmission characteristics. To study the transmission of the ion funnel, a BSA tryptic digest sample was directly infused into the IMS platform utilizing two buffer gas compositions in the source IFT: (1) 100% N_2/0% He and (2) 30% N_2/70% He. The drift cell in these experiments was filled with 100% N_2. As shown in Figure 2, the mass spectra at both gas compositions are virtually identical in terms of sensitivity and m/z distribution, indicating that He has no detectable effect on the performance of the IFT in continuous mode. However, when the trap was enabled, there was a dramatic effect on the mass spectra as shown in Figure 3. The results shown in Figure 3 were obtained using a trap injection
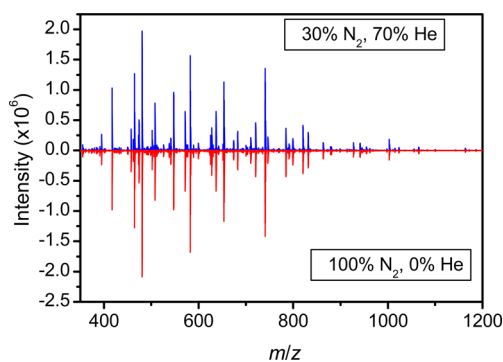

Figure 2. Comparison of mass spectra for ESI of a 0.2 μg/μL bovine serum albumin (BSA) tryptic digest while operating the IMS-MS in transmission mode (no trapping) utilizing two different gas compositions.
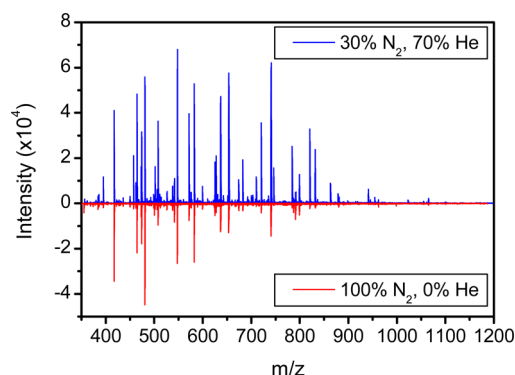
Figure 3. Mass spectra of BSA tryptic digest while operating the IFT of the IMS-MS in trapping mode utilizing two different gas compositions. Trapping time is 3.24 ms while the trap exit gate is 480 μs.

time of 3.24 ms and ejection pulse of 480 μs. The most prominent difference in the mass spectra when He was added to N_2 is higher intensity for most of the peaks, especially higher m/z peaks (>m/z 500). The signal improvements for higher m/z species were generally more than an order of magnitude. A possible reason for the observed high intensities is the faster release of ions which otherwise were slow to leave the trap within 480 μs. To investigate the effect of the increased ion release speed in the presence of He, the gate opening time (i.e., ion ejection time) was varied from 160 to 1800 μs (while keeping the trapping injection time constant at 3.24 ms) to see when all of the ions exited the trap. Shown in Figure 4a are the intensities for three peaks as a function of exit gate opening time. The intensity of ions reached their maximum in He within ~800 μs. Their intensities were also observed to be higher than in pure N_2 for the same gate opening time indicating that ions are released from the trap faster in a 70% He/30% N_2 gas mixture than in 100% N_2. It should be noted that the plateau observed in Figure 4 is not due to ADC saturation as the intensity values were below the saturation level of the ADC. The plateau observed in Figure 4 is most likely due to better evacuation of the ions from the trap in the case of He. Faster ejection from the trap should depend on the mobility of ions, or in other words, ions of low mobility should show the greatest improvement upon adding He while those ions of high mobility should have the least improvement. As shown in Figure 4a, the difference in sensitivity between 70% N_2/30% He and 100% N_2 is on the order of 784.38 (2+) > 831.38 (3+) > 571.86 (2+) which correlates with mobilities of 571.86 > 831.38 > 784.38 (Figure 4b). In other words, ions of low mobility (784.38 (2+)) showed the greatest improvement in sensitivity upon using He. The improvement in sensitivity observed in Figure 4a ranges from a factor of 12 to 18 for a 480 μs gate opening time. Importantly, this improvement in sensitivity was observed for the small gate opening times that are typically mandated in IMS measurements for optimum resolving power. The results shown in Figure 4 are consistent with the higher mobility of ions in He than in N_2. Since the mobility of ions K is defined as[1]

$$K = \frac{3ze}{16N}\sqrt{\frac{2\pi}{\mu kT}}\frac{1}{\Omega}$$

where ze is the ion charge, N is the number density, μ is the reduced mass of the ion-neutral pair, k is Boltzmann's constant, T is temperature, and Ω is the collision cross section. Since μ is
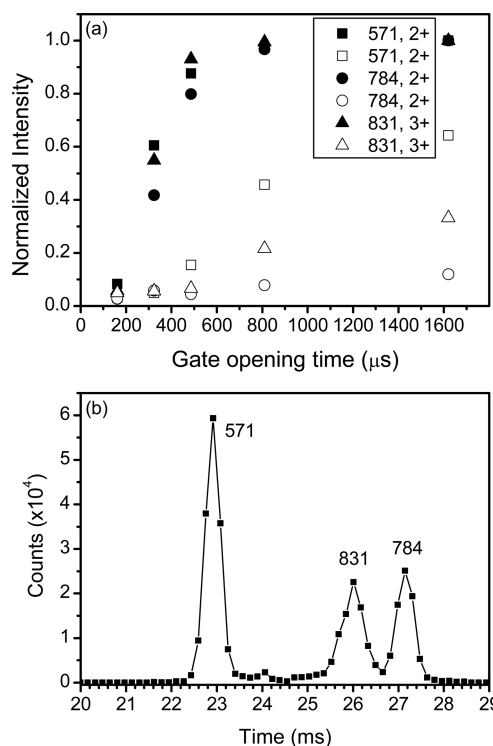

Figure 4. (a) Normalized intensities of monoisotope mass for three peaks as a function of gate opening time at trap injection time of 3.24 ms. Solid symbols are for 30% N_2/70% He while open symbols are for 100% N_2/0% He. For clarity, intensities are normalized to the highest value for each ion. (b) Arrival time distribution of three peaks at m/z 571, 784, and 831 collected utilizing 480 μs gate opening time for 30% N_2/70% He buffer gas composition.

~7 times smaller for the ion-He than the ion-N_2 pair and Ω of peptides is ~35% smaller in He than in N_2,[15] the mobility of ions is higher in He than in N_2. However, the intensities for 784.38 (2+) and 831.38 (3+) in 100% N_2 do not reach the intensities in the 70% He/30% N_2 gas mixture even for a long gate opening time of 1.62 ms. One reason could be a more diffuse ion packet inside the trap in the case of N_2 requiring more than 1.6 ms to fully exit. Another reason could be some undetermined mechanism of ion loss that is greater in N_2 than in He. Another possibility for the difference between nitrogen and helium could be a difference in the effective trapping of ions for the different gas compositions. The effective potential barrier confining ions in the radial direction changes with the buffer gas conditions according to the factor γ.[16]

$$\gamma = \frac{\omega^2\tau^2}{1 + \omega^2\tau^2}$$

Here, ω is the RF frequency expressed in angular units, $\omega = 2\pi f$; the ion velocity collisional relaxation time τ is related to the ion mobility K:

$$\tau = \frac{m}{ze}K$$

Here, m is ion mass and ze is the charge. The ion mobility in He is ~3.5 times higher than in N_2;[15] hence, the relaxation time for He is also increased by the same factor. It follows that the gas composition term γ is higher for He buffer gas, compared to the pure N_2 case. For pressure conditions here, P = 4 Torr, and RF frequency f = 1.0 MHz, we obtain for He γ = 0.96 and for

N_2 $\gamma = 0.65$, indicating only a minor reduction of the effective potential barrier due to the buffer gas in each case. Measurements here were taken under conditions when the IFT was not "overfilled", such that a minor variation of the effective potential did not create a measurable difference. However, the difference in γ is more significant for increased buffer gas pressures, e.g., $P > \sim 10$ Torr;[17] thus, optimizing RF frequency and voltage for a specific gas composition would be beneficial at the higher pressure.

To aid in understanding the trap behavior in He and in N_2, we simulated the IFT operation using SIMION 8.1. Ions of 784 (2+) m/z were trapped inside the IFT for 2 ms and then ejected from the trap using a gate opening time of 480 μs. During the 2 ms trapping period, there were no losses of ions to the trap for either buffer gas composition, indicating similar trapping efficiencies. However, as the ions exit the trap in both gases, some ions were lost to the electrodes immediately following the exit gate (the converging section) while some ions did not exit the trap (i.e., were retained) as shown in Figure 5. In N_2 buffer gas, 44% of ions are retained in the trap
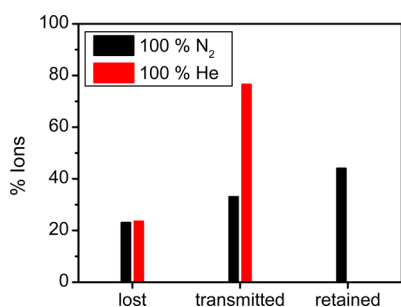

Figure 5. Ion simulation results for the IFT for two buffer gas compositions. Black: 100% N_2; red: 100% He.

without being ejected, while no ions were retained using the He buffer gas indicating better ejection efficiency for the He. Losses for N_2 gas were much greater with only 33% of ions transmitted while 77% were transmitted in He with losses of 23% for both N_2 and He in the converging section. This is in line with the experimental observations (Figure 4) and further illustrates why He-enriched buffer gas improves signal intensity. Ion simulations further supported that the performance of the IFT is improved in the He-enriched buffer gas relative to pure N_2 and that most of the improvement comes from faster ion ejection. The ion simulations also provide insight into further improving the performance of the IFT by minimizing ion losses in the converging region. During trapping, the ion cloud expands and ions are trapped in regions close to the ring electrodes of the trap. The exit gate DC potential pushes the ions closer to the IFT ring electrodes due to the DC field penetration and upon release from the trap, and these ions are not immediately refocused to the center. Therefore, they are more prone to be lost to the electrodes (as revealed from simulations) in the converging section of the IFT that immediately follows the exit gate. One possible modification to address ion losses at the converging section would be to keep the inner diameter constant for the first few electrodes following the trapping section before forming a converging shape. This would allow the ions to refocus to the center prior to entering the converging section of the funnel. Indeed, SIMION simulations indicate that only 1% of ions are lost in such an IFT design utilizing N_2 as compared to 23% in the

current design (Figure 5). Experimental verification of this change to the IFT design is planned.

The introduction of He into the trapping region of the IFT can also lead to leakage of He into the drift cell. This leakage causes ion arrival times to shift to shorter values based upon helium composition which may result in reduced IMS resolving power in the present IMS-MS design since $R = t/\Delta t$, where t is arrival time and Δt is the peak width at full width half-maximum. To explicitly investigate the He effect on the IMS resolving power, we introduced the same He/N_2 gas mixture into both the ion source and drift cell by splitting the gas mixture supply line (Figure 1), making the gas composition in the source identical to that in the drift cell. As expected, as the He composition increased, the arrival time decreased linearly. In some cases, the calculated IMS resolving power (Figure 6) slightly improved upon adding He, but in others, the resolving power did not change. Thus, benefits of He as a buffer gas in both the trap and drift cell were observed since it did not degrade the IMS resolving power, allowed a somewhat
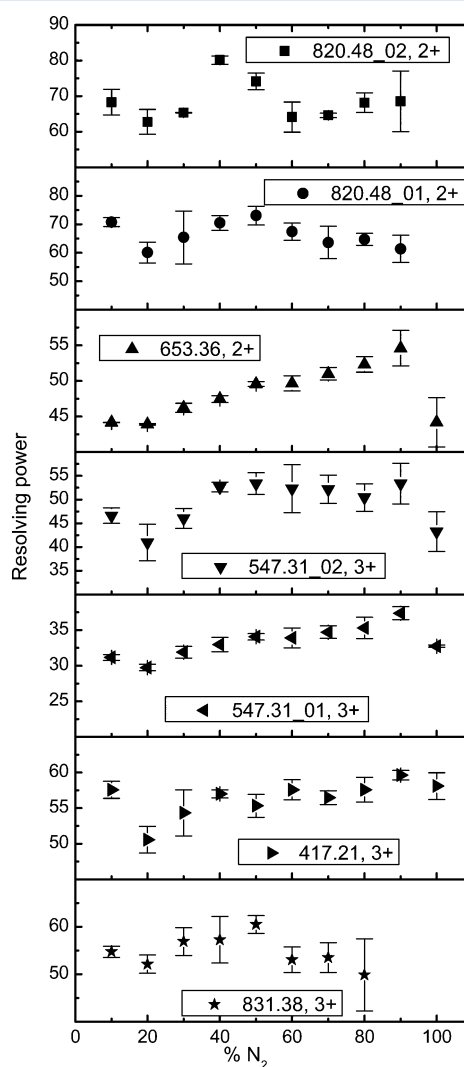

Figure 6. Measured IMS resolving power for several ions from ESI of a BSA tryptic digest as a function of nitrogen percentage in a N_2/He buffer gas mixture. Several ions have two conformers and they are reported separately. Trap injection time was maintained at 3.24 ms while the gate opening time was 480 μs.

increased duty cycle, and resulted in greatly improved signal intensities with the present design.

CONCLUSIONS

We have observed that utilizing helium in the ion funnel trap during ion ejection improves the sensitivity of our IMS-MS platform by more than an order of magnitude for lower mobility ions. The improvement in sensitivity is attributed primarily to the faster ejection of ions from the ion funnel trap, which was confirmed by ion simulations using SIMION. To a much lesser degree, the improvements in sensitivity can be attributed to better ion confinement in He relative to nitrogen. The ion ejection from the trap can be improved by lowering the pressure in the trap. Thus, the effects observed in this work may not be as dramatic for traps that operate at lower pressure. The IMS platform used in this work utilizes a trap that works at a similar pressure as the drift cell. This arrangement maximizes the sensitivity by drastically minimizing ion losses at the interface between the trap and the drift cell, as well as minimizing ion activation during transport to the drift cell. However, traps that operate at lower pressure (mTorr) are often coupled to drift cells operating at higher pressures (e.g., a few torr). The large pressure difference (more than an order of magnitude) between the trap and the drift cell creates a significant challenge for injecting ions. Conformational change as well as ion activation has been attributed to higher injection voltages.[18] In addition, in the absence of effective ion confinement at the trap/drift cell interface, ion losses are inevitable. Ion activation in IMS platforms that utilized this large pressure difference between the trap and the drift cell has been reduced but not eliminated, by inclusion of a helium rich region between the trap and the drift cell. In contrast, the IMS platform described here utilizes a much smoother and gradual change in pressure between the trap and the drift cell (∼50 mTorr) resulting in maximum ion transmission and minimal ion activation in nitrogen as well as in helium. Although a goal of this work was to evaluate possible improvements in sensitivity of IMS-MS measurements, a specific instrument platform was used that incorporated only a one source ion funnel. Since ESI in an environment that is highly rich in He can be problematic due to electrical breakdown phenomena, utilizing a dual funnel interface[17] is advantageous for allowing independent control over the gas composition of the ESI interface and IFT-drift tube regions. Finally, the present work suggests modifications that should result in further improvements to IMS-MS performance.

ASSOCIATED CONTENT

Ⓢ Supporting Information

Additional information as noted in text. This material is available free of charge via the Internet at http://pubs.acs.org/

AUTHOR INFORMATION

Corresponding Author

*E-mail: yehia.ibrahim@pnnl.gov. Telephone: 509-371-6526. Fax: 509-371-656.

Notes

The authors declare no competing financial interest.

ACKNOWLEDGMENTS

REFERENCES

(1) Mason, E.; McDaniel, E. *Transport Properites of Ions in Gases*; Wiley: New York, 1988.

(2) Revercomb, H. E.; Mason, E. A. *Anal. Chem.* **1975**, *47*, 970−983.

(3) Tang, K.; Shvartsburg, A. A.; Lee, H. N.; Prior, D. C.; Buschbach, M. A.; Li, F. M.; Tolmachev, A. V.; Anderson, G. A.; Smith, R. D. *Anal. Chem.* **2005**, *77*, 3330−3339.

(4) Howdle, M. D.; Eckers, C.; Laures, A. M. F.; Creaser, C. S. *Int. J. Mass Spectrom.* **2010**, *298*, 72−77. Ruotolo, B. T.; McLean, J. A.; Gillig, K. J.; Russell, D. H. *J. Mass Spectrom.* **2004**, *39*, 361−367. Asbury, G. R.; Hill, H. H. *Anal. Chem.* **1999**, *72*, 580−584. Matz, L.; Hill, H.; Beegle, L.; Kanik, I. *J. Am. Soc. Mass Spectrom.* **2002**, *13*, 300−307.

(5) Gillig, K. J.; Ruotolo, B.; Stone, E. G.; Russell, D. H.; Fuhrer, K.; Gonin, M.; Schultz, A. J. *Anal. Chem.* **2000**, *72*, 3965−3971.

(6) Wittmer, D.; Chen, Y. H.; Luckenbill, B. K.; Hill, H. H. *Anal. Chem.* **1994**, *66*, 2348−2355.

(7) Bradbury, N. E.; Nielsen, R. A. *Phys. Rev.* **1936**, *49*, 388.

(8) Zhou, L.; Collins, D. C.; Lee, E. D.; Lee, M. L. *Anal. Bioanal. Chem.* **2007**, *388*, 189−194.

(9) Hoaglund, C. S.; Valentine, S. J.; Clemmer, D. E. *Anal. Chem.* **1997**, *69*, 4156−4161. Myung, S.; Lee, Y. J.; Moon, M. H.; Taraszka, J.; Sowell, R.; Koeniger, S.; Hilderbrand, A. E.; Valentine, S. J.; Cherbas, L.; Cherbas, P.; Kaufmann, T. C.; Miller, D. F.; Mechref, Y.; Novotny, M. V.; Ewing, M. A.; Sporleder, C. R.; Clemmer, D. E. *Anal. Chem.* **2003**, *75*, 5137−5145. Creaser, C. S.; Benyezzar, M.; Griffiths, J. R.; Stygall, J. W. *Anal. Chem.* **2000**, *72*, 2724−2729.

(10) Clowers, B. H.; Ibrahim, Y. M.; Prior, D. C.; Danielson, W. F., 3rd; Belov, M. E.; Smith, R. D. *Anal. Chem.* **2008**, *80*, 612−623.

(11) Tang, K.; Shvartsburg, A. A.; Lee, H. N.; Prior, D. C.; Buschbach, M. A.; Li, F.; Tolmachev, A. V.; Anderson, G. A.; Smith, R. D. *Anal. Chem.* **2005**, *77*, 3330−3339.

(12) Ibrahim, Y. M.; Belov, M. E.; Tolmachev, A. V.; Prior, D. C.; Smith, R. D. *Anal. Chem.* **2007**, *79*, 7845−7852.

(13) Appelhans, A. D.; Dahl, D. A. *Int. J. Mass Spectrom.* **2005**, *244*, 1−14.

(14) Kinter, M. M.; Sherman, N. E. *Protein Sequencing and Identification Using Tandem Mass Spectrometry*; Wiley-Interscience: New York, 2000.

(15) Bush, M. F.; Campuzano, I. D. G.; Robinson, C. V. *Anal. Chem.* **2012**, *84*, 7124−7130.

(16) Tolmachev, A. V.; Chernushevich, I. V.; Dodonov, A. F.; Standing, K. G. *Nucl. Instrum. Methods Phys. Res., Sect. B: Beam Interact. Mater. Atoms* **1997**, *124*, 112−119.

(17) Ibrahim, Y.; Tang, K.; Tolmachev, A. V.; Shvartsburg, A. A.; Smith, R. D. *J. Am. Soc. Mass Spectrom.* **2006**, *17*, 1299−1305.

(18) Shelimov, K. B.; Clemmer, D. E.; Hudgins, R. R.; Jarrold, M. F. *J. Am. Chem. Soc.* **1997**, *119*, 2240−2248. Merenbloom, S. I.; Flick, T. G.; Williams, E. R. *J. Am. Soc. Mass Spectrom.* **2012**, *23*, 553−562.